SLIP LINE METHOD FOR SINTERED POWDER MATERIALS UNDER CONDITION OF AXIAL SYMMETRY DEFORMATION①

Zhao, Zhongzhi Hua, Lin
Wuhan Institute of Technology, Wuhan 430070, China

ABSTRACT

Slip line method for sintered powder materials under condition of axial symmetry is proposed based on the simplified yield condition of sintered powder materials and Haar-von Karman perfect plastic criterion. The equations of slip line and stress along slip line are derived, and numerical solutions are given. Deformation load in closed die upsetting of sintered copper cylinder is calculated by slip line method, and theoretical solutions are compared with experimental results.

Key word: sintered powder material axial symmetry deformation slip line method

1 INTRODUCTION

Plastic working is an important technology in production of high performance parts of sintered powder materials. In the plastic deformation of sintered powder materials, not only the form of the preform is changed but also the volume of the preform is changed greatly, therefore the classical plasticity theory based on the volume constancy can not be applied to analyse the deformation of sintered powder materials directly. The research of plasticity theory for sintered powder materials has been made since 1970's in order to guide the technological design of its plastic working in theory, and important progress[1-4] on yield criterion and slip line theory in plane strain and so on. has been achieved. In the plastic working of sintered powder materials, e.g. extrusion, die forging etc of rotated body parts is a problem of axial symmetry deformation, the research of axial symmetry deformation for sintered powder materials is needed for practice. Slip line theory[5,6] for fully dense metal and soil in axial symmetry has been developed, the sintered powder materials are materials between fully dense metals and soils and similar to these two kinds of materials in deformation characteristics. Therefore the slip line method for sintered powder materials in axial symmetry is worthy of research.

2 SIMPLIFICATION OF YIELD CONDITION

The yield condition[1, 2, 7] of sintered powder materials is

$$3J_2 + (\alpha\sigma_m)^2 = Y^2 \qquad (1)$$

where J_2 —the second invariant of deviator stress tensor;

σ_m—hydrostatic pressure;

α —coefficient related to relative density of preform and $\alpha = 3\sqrt{1-\rho^2/2+\rho^2}$;

Y —equivalent yield strength of the

① Manusript received Nov. 12, 1992

sintered powder material

In the coordinates of principal stress (σ_1, σ_2, σ_3), the geometrical form of yield condition of expression (1) can be shown as an elliptic sphere. The characteristic lines from the differential equtions of equilibrum of stress in accordance with yield condition of expression (1) are not always of two groups of real solutions. In order to easily operate in mathematics, the hexagonal pyramid[3] in the elliptic sphere is used to express the yield surface of sintered powder materials approximately, then the simplified yield condition[3, 4] of sintered powder materials corresponding to the hexagonal pyramid is shown as follows

$$\left.\begin{aligned}\sigma_{max}-\sigma_{min}-(\sigma_{max}+\sigma_{min})\sin\theta=Y\cos\theta,\sigma_m\leqslant 0\\ \sigma_{max}-\sigma_{min}+(\sigma_{max}+\sigma_{min})\sin\theta=Y\cos\theta,\sigma_m>0\end{aligned}\right\}\quad(2)$$

where σ_{max}, σ_{min}—the maximum and the minimum principal stresses in algebraic value respectively; θ—function of coefficient α, $\theta=\mathrm{tg}^{-1}(\alpha/2)$.

The geometrical forms of yield condition of expression (1) and simplified yield condition of expression (2) are shown as Fig. 1. If the relative density of sintered powder material $\rho=1$, i. e. the sintered powder material is changed into fully dense material, then $\alpha=0$, $\theta=0$, expressions (1) and (2) are changed into Mises yield condition and Tresca yield condition of fully dense metal respectively, this indicates that the yield condition of fully dense material is only a special case of sintered powder material.

3 Haar-von Karman PERFECT PLASTIC CRITERION

In cylindrical coordinates (r, φ, z), the non-zero stresses in axial symmetry are σ_r, σ_φ, σ_z, τ_{rz}, they are functions of (r, z). For $\tau_{r\varphi}=\tau_{\varphi z}=0$, σ_φ is a principal stress. For the fully dense material in axial symmetry deformation Shield[5] analysed in detail

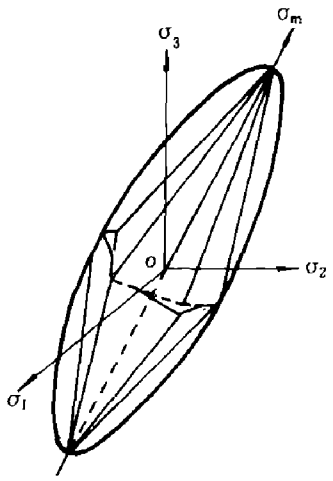

Fig. 1 The yield surface of sintered powder materials

the basic equations in each plastic stress state based on the Tresca yield condition, and pointed out that assuming σ_q equals one of the other principal stress is correct, this hypothesis is the Haar-von Karman perfect plastic criterion. If the order of the principal stresses in algebraic value is $\sigma_1\geqslant\sigma_2\geqslant\sigma_3$, then $\sigma_{max}=\sigma_1$, $\sigma_{min}=\sigma_3$, the Haar—von Karman perfect plastic criterion can be expressed as follows

$$\left.\begin{aligned}&\sigma_\varphi=\sigma_2=\sigma_1\\ \text{or}\quad&\sigma_\varphi=\sigma_2=\sigma_3\end{aligned}\right\}\quad(3)$$

In the research of limit load of the cylindrical foundation in the soil mechanics, Березанцев[6] obtained practical result based on the perfect plastic criterion. Therefore, Haar-von Karman perfect plastic criterion can be applied to sintered powder materials which are between fully dense metals and soils in axial symmetry.

4 SLIP LINE METHOD

4.1 *Concept of Slip Line*

Generally, in plastic working of the sintered powder mterials there is $\sigma_m<0$, so the deformation related to $\sigma_m<0$ is discussed.

Take $\sigma=(\sigma_{max}+\sigma_{min})/2=(\sigma_1+\sigma_3)/2$ and substitute it into expression (2), we

have

$$\sigma_m \leqslant 0,\ \sigma_1 - \sigma_3 - 2\alpha\sin\theta = Y\cos\theta \tag{4}$$

In the coordinates of (σ, τ), the geometrical curve of yield condition of expression (4) is shown as Fig. 2. In Fig. 2 the stresses at one point in plane (r, z) represented on Mohr' s circle O_1 are in accord with yield condition (4). The points A, B on Mohr' s circle indicate two yield planes corresponding to the stress state, the tangential directions of these yield planes are along α, β expressed in Mohr' s circle O_1 in Fig. 2. If sintered powder material is in plastic state, the directions of α, β in (r, z) plane can be determined by yield condition and Mohr' s stress circle, then we can construct two groups of curves field those are intersected on a plane of which the tangential direction of each point is in accord with the tangential direction of yield plane of the point in plane(r, z), this curves field is slip line field. From Fig. 2, stipulate the lines rotated ($\pi/4 - \theta/2$) from the maximum stress σ_1 clockwise and counterclockwise are slip line α and β respectively.

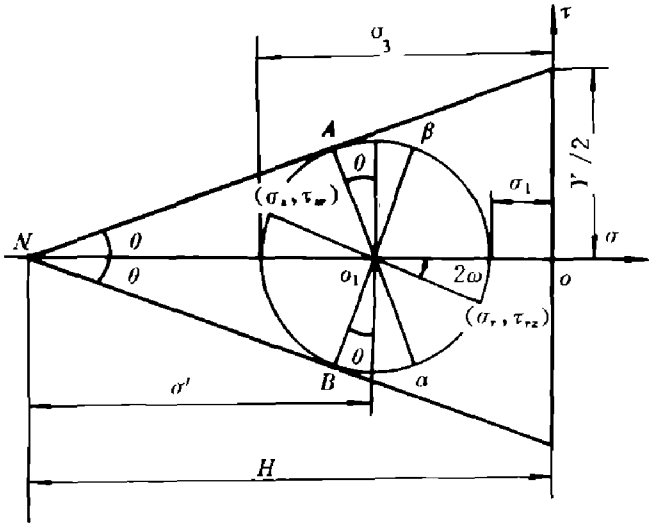

Fig. 2 Yield condition and Mohr's stress circle

4. 2 *Equations of Slip Line and Stress Along it*

(1) $\sigma_\varphi = \sigma_2 = \sigma_1$

In this case σ_φ is the maximum principal stress. In order to operate easily , take $H = Y/2\,\mathrm{ctg}\theta$, $\sigma' = H + 1/2(\sigma_1 + \sigma_3)$ and substitute them into expression (2), and from Fig. 2 we have

$$\left.\begin{aligned}\sigma_r &= \sigma'(1 + \sin\theta\cos2\omega) - H\\ \sigma_z &= \sigma'(1 - \sin\theta\cos2\omega) - H\\ \sigma_{rz} &= \sigma'\sin\theta\cos2\omega\\ \sigma_\varphi &= \sigma_1 = \sigma'(1 + \sin\theta) - H\end{aligned}\right\} \tag{5}$$

where ω is the angle rotating from coordinate r to the maximum stress σ_1 and take the angle of counter-clockwise as positive.

If we neglect volume stress, the differential equations of equilibrum[8] are

$$\left.\begin{aligned}&\frac{\partial\sigma_r}{\partial r} + \frac{\partial\sigma_{rz}}{\partial z} + \frac{\sigma_r - \sigma_\varphi}{r} = 0\\ &\frac{\partial\tau_{rz}}{\partial r} + \frac{\partial\sigma_z}{\partial z} + \frac{\tau_{rz}}{r} = 0\end{aligned}\right\} \tag{6}$$

Substitute expression(5) into(6) have

$$\left.\begin{aligned}&(1 + \sin\theta\cos2\omega)\frac{\partial\sigma'}{\partial r} + \sin\theta\sin2\omega\frac{\partial\sigma'}{\partial z}\\ &\quad - 2\sigma'\sin\theta\sin2\omega\frac{\partial\omega}{\partial r} + 2\sigma'\sin\theta\cos2\omega\frac{\partial\omega}{\partial z}\\ &= -\frac{\sigma'\sin\theta(-1 + \cos2\omega)}{r}\\ &\sin\theta\sin2\omega\frac{\partial\sigma'}{\partial r} + (1 - \sin\theta\cos2\omega)\frac{\partial\sigma'}{\partial z}\\ &\quad + 2\sigma'\sin\theta\cos2\omega\frac{\partial\omega}{\partial r} + 2\sigma'\sin\theta\sin2\omega\frac{\partial\omega}{\partial z}\\ &= -\frac{\sigma'\sin\theta\sin2\omega}{r}\end{aligned}\right\} \tag{7}$$

The characteristic equations from expression (7) are as follows.

$$\left.\begin{aligned}&\mathrm{d}z = \mathrm{tg}(\omega - \omega_0)\mathrm{d}r\\ &\mathrm{d}\left(\frac{1}{2}\mathrm{ctg}\theta\ln\frac{\sigma + \frac{1}{2}Y\mathrm{ctg}\theta}{\sigma_0} - \omega\right)\\ &= \frac{\sin(\omega - \omega_0) + \sin(\omega + \omega_0)}{2r\cos(\omega - \omega_0)}\mathrm{d}r\end{aligned}\right\} \tag{8a}$$

$$\left.\begin{aligned}&\mathrm{d}z = \mathrm{tg}(\omega + \omega_0)\mathrm{d}r\\ &\mathrm{d}\left(\frac{1}{2}\mathrm{ctg}\theta\ln\frac{\sigma + \frac{1}{2}Y\mathrm{ctg}\theta}{\sigma_0} + \omega\right)\\ &= -\frac{\sin(\omega - \omega_0) + \sin(\omega + \omega_0)}{2r\cos(\omega + \omega_0)}\mathrm{d}r\end{aligned}\right\} \tag{8b}$$

where $\omega_0 = \pi/4 - \theta/2$ and σ_0 is a stress constant.

From Fig. 3, we can obtain the differ-

ential equations of slip lines from their difinition as follows.

$$\left.\begin{aligned}&\text{slip line } \alpha\text{: } dz = \mathrm{tg}(\omega - \omega_0)dr\\&\text{slip line } \beta\text{: } dz = \mathrm{tg}(\omega + \omega_0)dr\end{aligned}\right\} \quad (9)$$

Comparing slip line equations (9) to characteristic line equations in the first expression of equations (8a) and (8b), we know the slip lines are the same as characteristic lines. If characteristic line field, i. e. slip line field is constructed, then the stress distribution in plastic zone of plane (r, z) can be determined from the characteristic equations.

(2) $\sigma_\varphi = \sigma_2 = \sigma_3$

In this case σ_φ is the minimum principal stress. According to the above method, we have characteristic equations as follows.

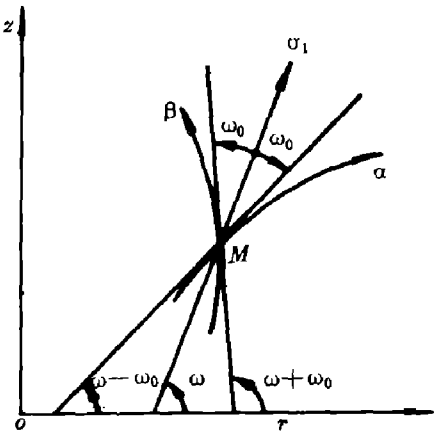

Fig. 3 Slip line and the maximum stress

$$\left.\begin{aligned}&dz = tg(\omega - \omega_0)dr\\&\mathrm{d}\left(\frac{1}{2}\,\mathrm{ctg}\theta \ln\frac{\sigma + \frac{1}{2}Y\,ctg\theta}{\sigma_0} - \omega\right)\\&= \frac{\sin(\omega - \omega_0) - \sin(\omega + \omega_0)}{2r\cos(\omega - \omega_0)}dr\end{aligned}\right\} \quad (10a)$$

$$\left.\begin{aligned}&\mathrm{d}z = \mathrm{tg}(\omega + \omega_0)\mathrm{d}r\\&\mathrm{d}\left(\frac{1}{2}\,\mathrm{ctg}\theta \ln\frac{\sigma + \frac{1}{2}Y\,\mathrm{ctg}\theta}{\sigma_0} + \omega\right)\\&= \frac{\sin(\omega - \omega_0) - \sin(\omega + \omega_0)}{2r\cos(\omega + \omega_0)}dr\end{aligned}\right\} \quad (10b)$$

5 NUMERICAL SOLUTIONS OF CHARACTERISTIC EQUATIONS

The analytic solutions of equations (8), (10) can not be obtained generally, then the numerical method (finite difference method is used in the paper) must be applied to solve them. See Fig. 4, take i, j as the numbers of α, β and substitute finite difference for differential of equations (8), (10), we have

(1) $\sigma_\varphi = \sigma_z = \sigma_1$

$$\left.\begin{aligned}&r[i,j] = \left\{\begin{aligned}&r[i,j-1]\mathrm{tg}(\omega[i,j-1] - \omega_0) - r[i-1,j]\\&\times \mathrm{tg}(\omega[i-1,j] + \omega_0) - z[i,j-1] + z[i-1,j]\end{aligned}\right.\\&\div \{\mathrm{tg}(\omega[i,j-1] - \omega_0) - \mathrm{tg}(\omega[i-1,j] + \omega_0)\}\\&z[i,j] = z[i,j-1] + (r[i,j]\\&- r[i,j-1])\mathrm{tg}(\omega[i,j-1] - \omega_0)\\&\omega[i,j] = \frac{1}{2}(F_2 - F_1 + \omega[i,j-1] + \omega[i-1,j]\\&+ \frac{1}{2}\,\mathrm{ctg}\theta \ln\frac{\frac{Y}{2}\,\mathrm{ctg}\theta + \sigma[i-1,j]}{\frac{Y}{2}\,\mathrm{ctg}\theta + \sigma[i,j-1]})\\&\sigma[i,j] = (\sigma[i,j-1] + \frac{Y}{2}\,\mathrm{ctg}\theta)\exp(2\,\mathrm{tg}\theta \times\\&\times (F_1 + \omega[i,j] - \omega[i,j-1])) - \frac{Y}{2}\,\mathrm{ctg}\theta\end{aligned}\right\} \quad (11a)$$

where

$$\left.\begin{aligned}&F_1 = \frac{sin(\omega[i,j-1] + \omega_0) + sin(\omega[i,j-1] - \omega_0)}{2r[i,j-1]cos(\omega[i,j-1] - \omega_0)}\\&\times (r[i,j] - r[i,j-1])\\&F_2 = -\frac{sin(\omega[i-1,j] + \omega_0) + sin(\omega[i-1,j] - \omega_0)}{2r[i-1,j]cos(\omega[i-1,j] + \omega_0}\\&\times (r[i,j] - r[i,j-1])\end{aligned}\right\} \quad (11b)$$

(2) $\sigma_\varphi = \sigma_2 = \sigma_3$

The finite difference solutions in this case are the same as expression (11a), but the F_1 and F_2 of expression (11a) must be changed into F'_1 and F'_2 respectively, the expressions of F'_1 and F'_2 are as follows

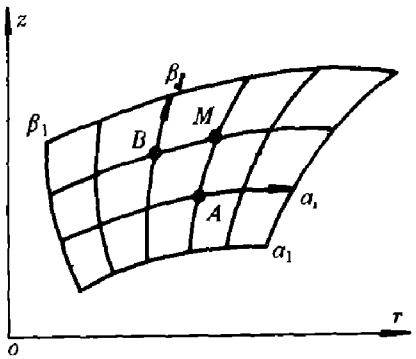

Fig. 4 General slip line field

$$\left.\begin{aligned}&F'_1 = \frac{\sin(\omega[i,j-1] - \omega_0) - \sin(\omega[i,j-1] + \omega_0)}{2r[i,j-1]\cos(\omega[i,j-1] - \omega_0}\\&\times (r[i,j] - r[i,j-1])\\&F'_2 = \frac{\sin(\omega[i-1,j] - \omega_0) - \sin(\omega[i-1,j] + \omega_0}{2r[i-1,j]\cos(\omega[i-1,j] + \omega_0)}\\&\times (r[i,j] - r[i-1,j])\end{aligned}\right\} \quad (12)$$

In order to improve the precision of finite difference solutions, the initial numerical solutions must be revised two or three times in the calculation as follows.

$$\left.\begin{aligned} S[i, j-1] &= (S[i, j] + S[i, j-1])/2 \\ S[i-1, j] &= (S[i, j] + S[i-1, j])/2 \end{aligned}\right\} \quad (13)$$

For expression (13), substitute r, z, ω, σ for S respectively in finite difference calculation.

6 SLIP LINE SOLUTION FOR CLOSED DIE UPSETTING OF SINTERED COPPER

6.1 *Theoretical Calculation*

Closed die upsetting is shown as Fig. 5, and in deformation there is $\sigma_\varphi = \sigma_2 = \sigma_1$[5]. Because of symmetry, it is enough to analyse the deformation of a quarter zone of preform. Consider two boundary conditions, i. e. no friction and there is a maximum friction applied on the contact surfaces of the punch and the preform, respectively, then the models of their slip line fields are shown as Fig. 5 (a) and (b) respectively. Each zone of the slip line model represents one of three boundary problems. The computation programs for constructing slip line field are based on the characteristics of each boundary problem, therefore, we can construct slip line field from free boundary AB, and determine stress distribution in plastic zone, furthermore the punch load can be calculated from the stress distribution in plastic zone. The equivalent yield strength Y of sintered powder material is needed in theoretcal calculation, so the uniaxial compression of cylinder specimen made from sintered powder material has been made to determine the equivalent yield strength Y. In uniaxial compression of cylinder there are $\sigma_r = \sigma_\varphi = \sigma_1 = 0$, $\sigma_z = \sigma_3 = -\sigma_s$, Substitute them into expression (4) and rearrange, then

$$Y = \left(\sqrt{1 + \frac{\alpha^2}{4}} + \frac{\alpha}{2}\right)\sigma_s \quad (14)$$

where σ_s is yield strength of sintered powder material in uniaxial compression. For sintered copper, its σ_s[7] can be expressed as follows.

$$\left.\begin{aligned} \sigma_s &= A\left(\ln \frac{\rho}{\rho_0}\sqrt{\frac{1-\rho_0^2}{1-\rho^2}}\right)^n \\ A &= -196.81 + 656.69\rho_0 (\mathrm{MPa}) \\ n &= 0.9031 - 0.6171\rho_0 \end{aligned}\right\} \quad (15)$$

where ρ_0 is initialy relative density of the sintered copper preform.

Slip line field of the closed die upsetting and compressive stress distribution on punch end calculated based on the slip line theory are show in Fig. 6 and Fig. 7 respectively.

6.2 *Experimental Results*

Experiments of closed die upsetting with sintered copper cylinder have been carried out to verify the theoretical calculation of slip line method. Cylindrical specimens were made from elctrolytic powder copper (purity of Cu≥99.8wt.-%) by a process of blending, compacting and sintering. The sintering atmosphere was cracked ammonium, the sintering temperature was 920±10 C, the sintering time was 2 h. the test of closed die upsetting was conducted on a WI−60 type material test machine at room temperature. In order to minimize the friction of the contact surface between the specimen and the die, and simulate frictionless boundary condition, the contact surfaces of both the specimin and the die were ground and polished and smeared with a lubricating zinc stearate —alcohol paste. In order to increase the friction on the contact surface between specimen and punch and simulate the maximum friction boundary condition, the punch end contacted with the specimen was machined into rough surface and smeared with a powder

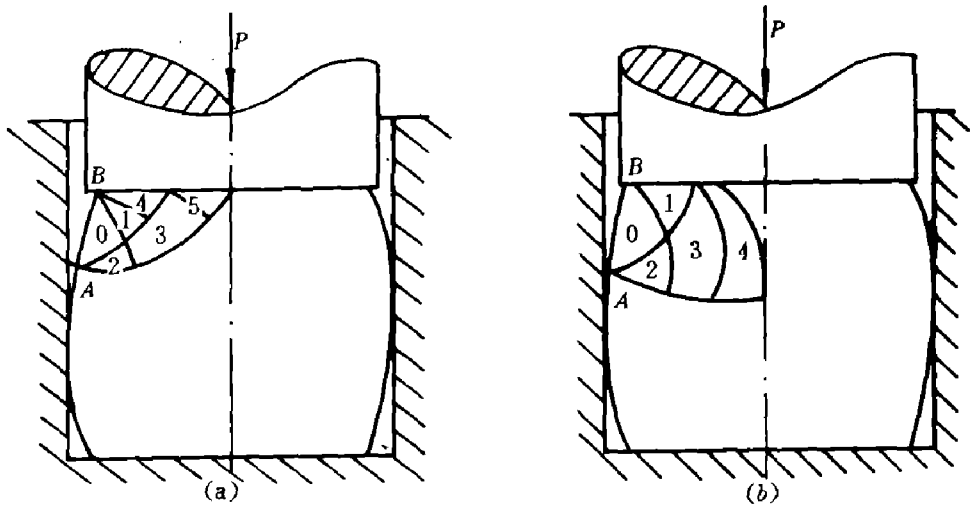

Fig. 5 Closed die upsetting and model of its slip line field
(a)—No friction on the contact surface between punch and peform;
(b)—The maximum friction on the contact surface between punch and preform

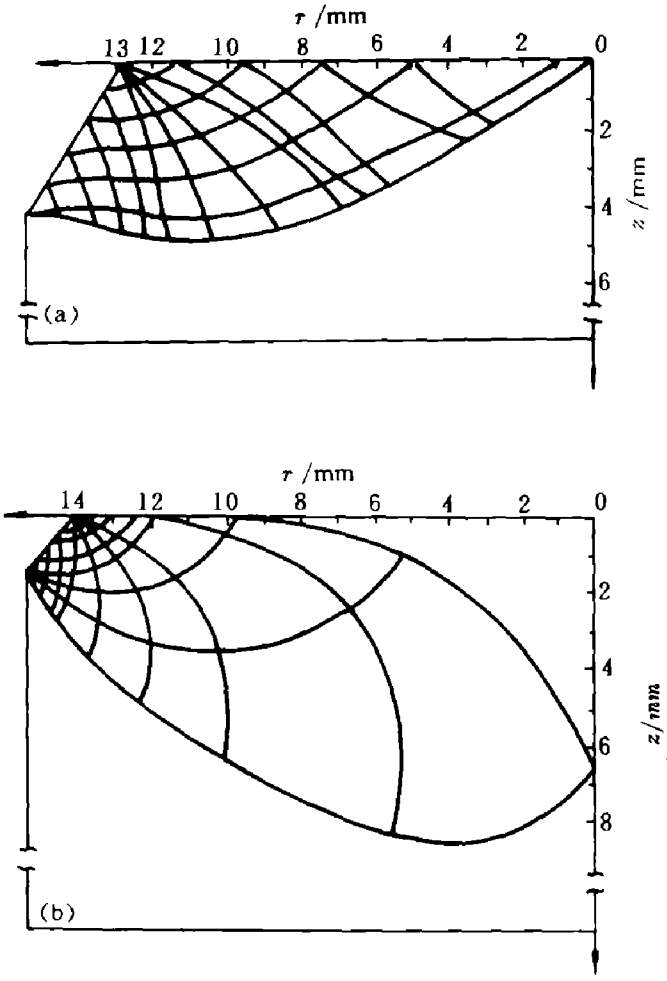

Fig. 6 Slip line field of closed die upsetting
(a)—No friction on contact surface between punch and preform; (b)—The maximum friction on contact surface between punch and preform

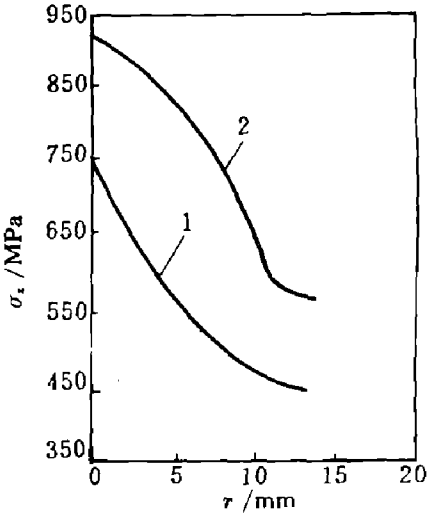

Fig. 7 Stress distribution on punch end
1—No friction on contact surface between punch and preform;
2—The maximum friction on contact surface between punch and preform

resin. The initial data of specimens are shown in Table 1.

The experimental and theoretical average punch Stresses are shown in Table 2. From Table 2, we know that theoretical average punch Stress is 20% or so lower than that of experiment with frictionless boundary condition, theoretical average punch stress is 4% and so higher than that of experiment

with maximum friction boundary, and this precision is admissible for technological design. In fact, the friction between punch and specimen can not be eliminated in test, so the experimental average punch stress is much higher than the theoretical value in the frictionless boundary condition. Because the maximum friction condition is in accord with practical testing condition, theoretical average punch stress is near to experimental value in the maximum friction boundary condition.

Table 1 Initial data of specimens for closed die upsetting

No	weight/g	diameter /mm	height /mm	relative density *
1	161.6	26.64	37.72	0.8508
2	209.1	29.23	40.84	0.8587

* Let the density of fully dense material be equal to 1.

Table 2 Theoretical and experimental average punch stress of closed die upsetting

No	boundary condition	relative density after upsetting	σ_T /Mpa	σ_E /Mpa	$\frac{\sigma_T-\sigma_E}{\sigma_E}$ /%
1	frictionless	0.9762	511	642	−20.4
2	maximum friction	0.9734	718	693	3.6

Notation: σ_T, σ_E are theoretical and experimental avevage punch pressures of closed die upsetting.

7 CONCLUSIONS

(1)Slip line method for sintered powder materials in axial symmetry is developed, equations (8) and (10) of slip line and stress along slip line are derived, and their finite difference solutions(11) are given;

(2)Slip line method for sintered powder materials in axial symmetry is applied to analyse closed die upsetting of sintered copper cylinder, theoretical average punch stress is in accordence with experimental value;

(3)Slip line method for sintered powder materials in axial symmety can be extended to analyse axial symmetry deformation of general compressible materials.

REFERENCES

1 Doraivelu, S M; Gegel, H L; Gunasekera, J S; Malas, J C; Morgan, J T. Int J Mech Sci, 1984, 26 (9/10): 527—535.

2 Hua, Lin; Zhao, Zhongzhi. Chinese J of Mechanical Eng, 1992, 28(4): 94—102.

3 大矢根守哉, 田端强. 塑性と加工, 1974, 15 (156): 43—51.

4 Zhao, Zhongzhi; Hua, Lin. Metal Forming Tech, 1985, (84): 10—19.

5 Shield, R T. On the plastic flow of metals under conditions of axial symmetry. Proc Roy Soc, 1955, A233: 267—287.

6 Березанцев, В Г. Расцт оснований сооружений. Изд. Литер. по Строт. 1970.

7 Hua, Lin; Zhao, Zhongzhi. Trans of Nonferrous Metals Society of China, 1992, 2(4): 82—87.

8 Wang, Ren; Xiong, Zhuhua; Huang, Wenbin. The foundations of plastic mechanics. Beijing: Science Press, 1982. 357.